International Journal of Applied Sciences and Smart Technologies

Volume 5, Issue 1, pages 101-112

p-ISSN 2655-8564, e-ISSN 2685-9432

A Brief on Optical-based Investigation towards The Interfacial Behaviors during High Viscous Liquid/Gas Countercurrent Two-Phase Flow in a Complex Conduit Representing 1/30 Down-Scaled of PWR Hot Leg Geometry

Achilleus Hermawan Astyanto[1, *], Indarto[2], Deendarlianto[2]

[1]*Department of Mechanical Engineering, Universitas Sanata Dharma, Kampus III USD Maguwoharjo, Yogyakarta 55282, Indonesia*

[2]*Department of Mechanical and Industrial Engineering, Universitas Gadjah Mada, Jalan Grafika No 2 Kampus UGM, Yogyakarta 55281, Indonesia*

[*]*Corresponding Author: achil.herma@usd.ac.id*

(Received 28-04-2023; Revised 04-05-2023; Accepted 04-05-2023)

Abstract

The present work briefly investigates liquid/gas countercurrent two-phase flow phenomena which can be specifically found in a mitigation during an accidental scenario in the operation of a nuclear reactor. A comprehensive knowledge on the corresponding phenomena is obviously important to avoid the failure on the cooling mechanism. Here, a pair of fluid containing high viscous liquid/gas flows through a complex conduit representing 1/30 scaled-down of PWR hot leg's typical geometry. Furthermore, the flow structures were visually observed, while the film thicknesses are extracted by an image processing algorithm through the corresponding optical-tabulated data. The obtained results reveal that a rather sharp decrease in liquid film corresponds to the flow regime transition.

Keywords: Countercurrent two-phase flow, liquid film thickness, high viscous liquid, complex conduit

1 Introduction

A gas/liquid countercurrent two-phase flow can be found in a mitigation of an accident on the operational of nuclear power plants. Here, it is strongly recommended that comprehensive knowledge on the corresponding phenomena is obviously important to avoid the failure on cooling mechanism during the scenario of loss of coolant accident because of a small break (SBLOCA) in the primary circuit of pressurized water reactors

(PWR). Furthermore, the database on the basis of analytical, mathematical, numerical and experimental investigations is able to elaborate the comprehensive behaviors of the corresponding flow phenomena [1].

Various studies have been carried out to investigate the characteristics of the flow structures during countercurrent two-phase flow. Visual observations are widely reported during the investigation on the basis of either large experimental works [2–5] or computational fluid dynamics [6]. Subsequently, measurement methods have also been developed to support the corresponding studies. Here, the studies on the pressure fluctuations were reported by several researches [7, 8]. Furthermore, the development of measurement methods has been conducted through physical measurements and also measurements on the basis of optical data. The concepts of conductance, capacitance and also impendence were largely reported as a particular technique during the measurements on the basis of electronic conceptions [9–13]. However, the characteristics of the flow regimes can be further obtained from the measurement on the basis of both the pressures and mainly interfacial behaviors since they strongly correspond to the fraction either the liquid or the gaseous phase, namely void fraction or liquid holdup, respectively.

On the other hand, the development of the measurements on the basis of optical data were introduced as well as the image processing techniques have been largely reported able to support the algorithm of object detections [14]. Therefore, since the interface between the phases during two-phase flow is defined as particular object, namely edge, the method may be used to support the description of a flooding which is initiated when the stability of the countercurrent flow cannot be maintained. Furthermore, the corresponding technique enables obtaining statistical characteristics of the countercurrent flow structures to be further elaborated as a regime identification method [15]. Here, various studies were conducted in both straight and complex geometries representing PWR hot leg’s typical geometry. Moreover, the corresponding development of measurement methods was then applied to investigate the effects of both geometry and fluid properties toward the characteristics of countercurrent flow.

From the aforementioned literature surveys, it is strongly implied that the interfacial behaviors during the visualization may establish practical advantages during the investigation on countercurrent flow. A further challenge to develop measurement

Volume 5, Issue 1, pages 101-112
p-ISSN 2655-8564, e-ISSN 2685-9432

techniques utilizing the optical data provides another opportunity to avoid such intrusive manners of conventional-physical measurements in which the probes should be contacted to the working fluids. Therefore, the present work elaborates the investigation of countercurrent flow phenomena on the basis of visual-optical data through the characteristics of liquid film thickness representing the interfacial behaviors.

2 Methods

Fig. 1 schematically depicts the experimental apparatus. The main components of the constructed facility which mainly represents a small scale of a primary circuit of PWR comprises simulators of a hot leg, a reactor pressure vessel (RPV) and a steam generator (SG). In an accordance with the supply systems of working fluids, a centrifugal water pump and a reciprocating air compressor are utilized to circulate the liquid and gas, respectively.

Table 1 provides the information of physical properties of the tested fluids. In order to increase the dynamic viscosity of the liquid, distilled water is mixed with glycerol in a percentage of 40% volume to total volume of the solution. On the other hand, to support the visual observations, a high speed video camera was utilized at 240 frame per second of recording rate.

Table 1. Physical properties of the tested fluids

Properties	**Gas**	**Liquid**
Density (kg/m^3)	1.15	1058.13
Dynamic viscosity (kg/m. s)	1.87×10^{-5}	31.67×10^{-4}
Surface tension (N/m)	-	0.064

Volume 5, Issue 1, pages 101-112

p-ISSN 2655-8564, e-ISSN 2685-9432

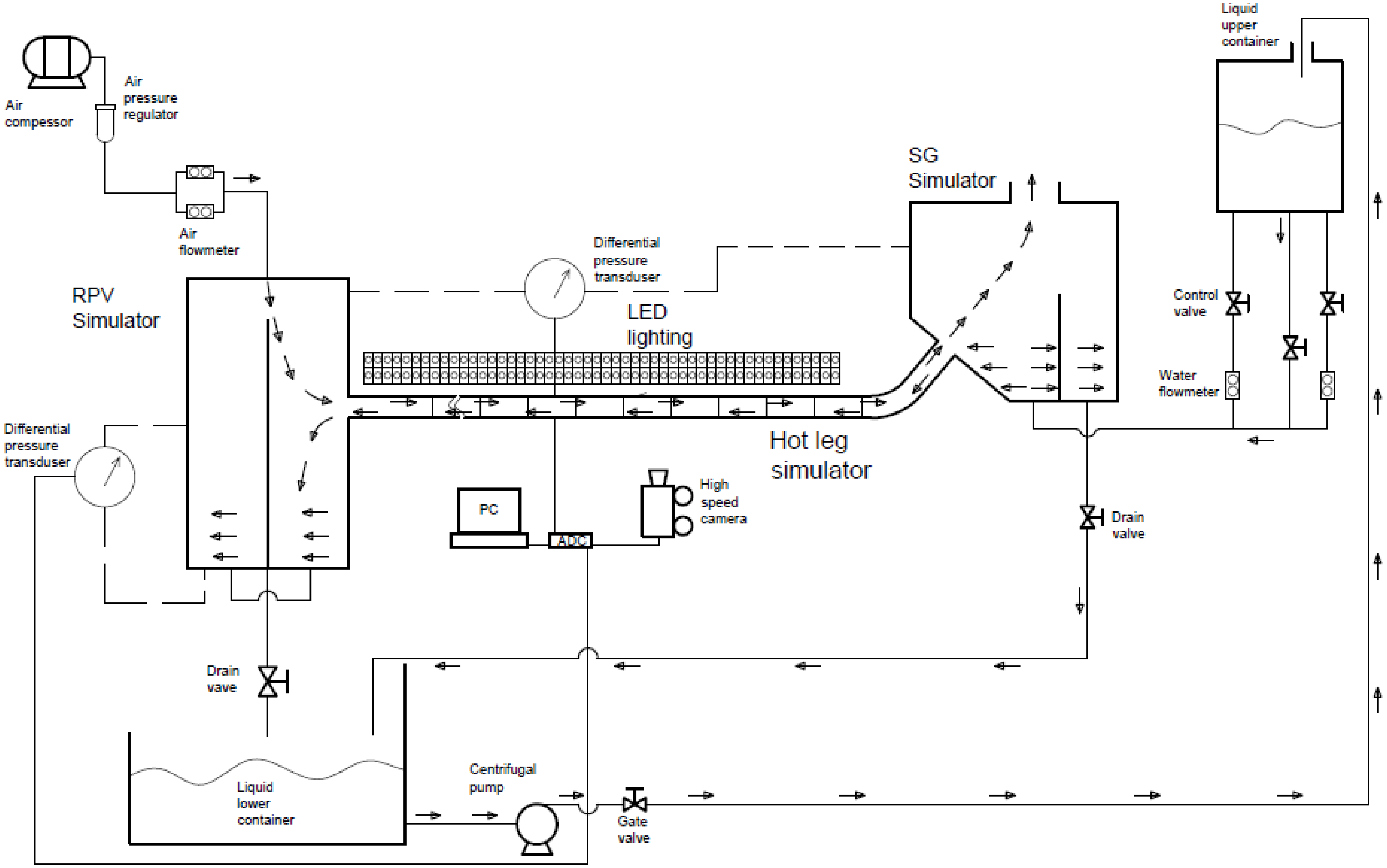

Figure 1. The scheme of experimental facility

International Journal of Applied Sciences and Smart Technologies
Volume 5, Issue 1, pages 101-112
p-ISSN 2655-8564, e-ISSN 2685-9432

In the present work, the flow parameters which comprise the liquid and gas flow rates were varied. For a constant flow rate of the liquid, the gas flow rate was increased stepwise by an increment of 5 liters per minute (lpm). On the other hand, when the gas flow rate is kept constant, the liquid flow rate was increased stepwise by an increment of 2 gallons per hour (gph). In addition, a rather detailed description regarding both the experimental apparatus and procedures can be found in Astyanto et al. [13].

Q_G (lpm)	Visual
10	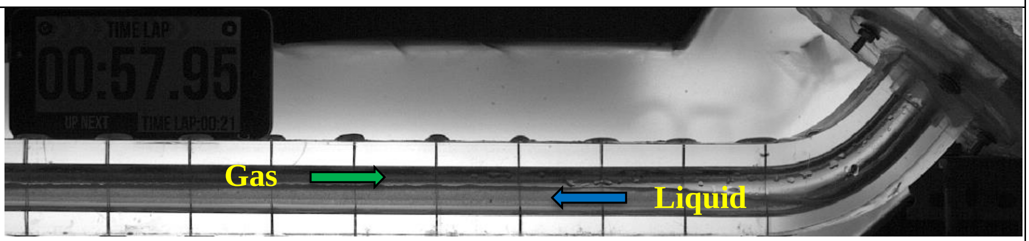
20	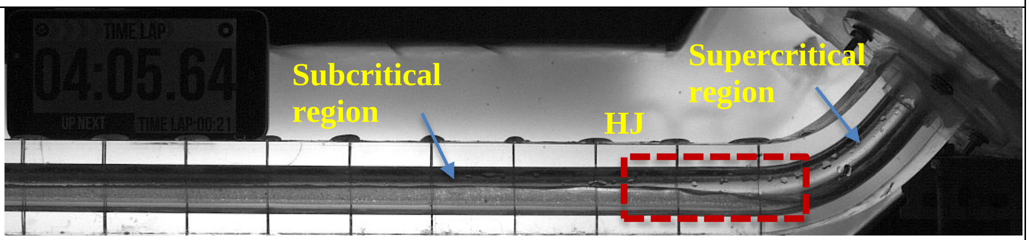
30	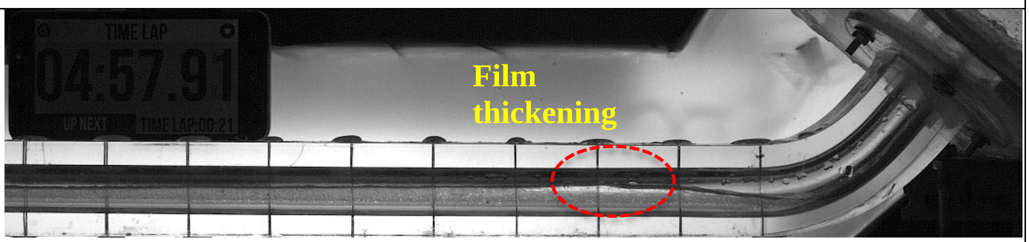

Figure 2. A typical set of visualization at the flow condition of Q_L= 24 gph with respect to the change of gas flow rate.

3 Results and Discussions

Fig. 2 shows a typical visualization of the countercurrent flow under a constant liquid flow rate, Q_L= 24 gph, with respect to the change of gas flow rate. From the figure it can be clearly seen that under this flow condition, a stratified structure is visually observed with a relatively stable interface on the lower gas flow rate. An inertial

International Journal of Applied Sciences and Smart Technologies
Volume 5, Issue 1, pages 101-112
p-ISSN 2655-8564, e-ISSN 2685-9432

dominated flow, namely supercritical flow, is observed in the inclined section and half of the elbow, while another gravitational dominated flow, i.e. subcritical flow, is observed in almost the entire horizontal section. A hydraulic jump (HJ) is further established as a flow transition from a supercritical to subcritical region. Here the liquid is accelerated by the presence of both riser's elevation and bended geometry. Moreover, as the gas flow rate is increased by a small increment, small waves are formed. They propagate along the direction of gas flow. As a result, a wavier interface followed by thickening film layer around the upper end of the hydraulic jump is further observed as the gas flow rate increases.

<table>
<tr><th>Q_L (gph)</th><th>Visual</th></tr>
<tr><td>16</td><td>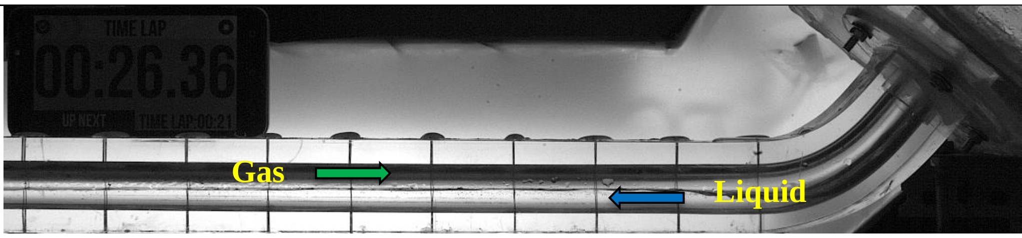
</td></tr>
<tr><td>20</td><td>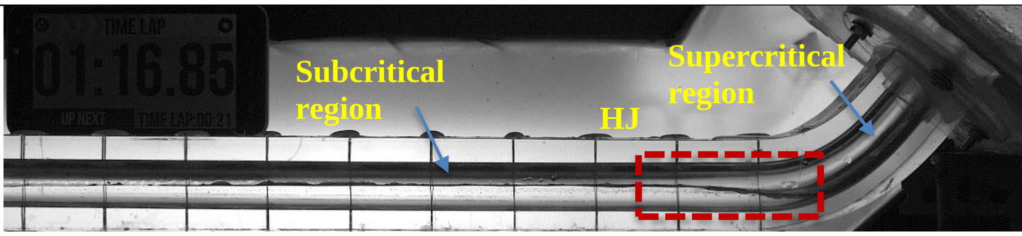
</td></tr>
<tr><td>24</td><td>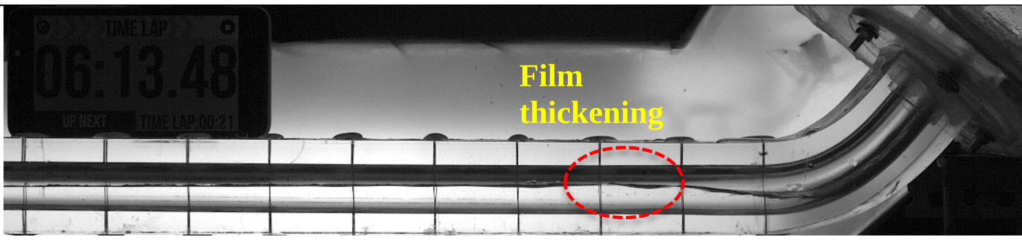
</td></tr>
</table>

Figure 3. Another typical set of flow visualization at the flow condition of Q_G= 30 lpm with respect to the change of liquid flow rate.

On the other hand, Fig. 3 depicts another typical visualization of the countercurrent flow under a constant liquid flow rate, Q_G= 30 lpm, with respect to the change of the liquid flow rate. From the figure it can be seen that under this flow condition, a stratified

Volume 5, Issue 1, pages 101-112
p-ISSN 2655-8564, e-ISSN 2685-9432

structure is also established with a rather fluctuate interface than the previous on the lower liquid flow rate when the liquid flow rate is kept constant. A supercritical flow is observed in the inclined section and half of the elbow, while a subcritical flow is observed in almost the entire horizontal section. Since in the beginning a lower liquid flow rate is applied here, a hydraulic jump with a shorter length is observed as its transition as the liquid is accelerated. Furthermore, as the liquid flow rate is increased, small waves are formed and propagate along the direction of gas flow. Similarly, a wavier interface with a thickening layer around the upper end of hydraulic jump is further observed as the liquid flow rate increases.

Fig. 4 shows the effect of gas flow rate towards the average of normalized film thickness, δ/D, under the flow condition of Q_L= 24 gph at several measurement coordinates (locus; L5, L6 and L7) of the subcritical region. From the figure it can be seen that δ/D slightly increases then decreases as the gas flow rate increases. From Q_G= 0 – 15 lpm, δ/D slightly increases in which the measurement location nearest the elbow obtains the thickest liquid film. Subsequently, from Q_G= 15 – 20 lpm L5, L6 and L7 exhibit an equal δ/D, whereas from Q_G= 20 – 35 lpm, δ/D decreases in which the measurement location nearest the elbow exhibits the sharpest slope.

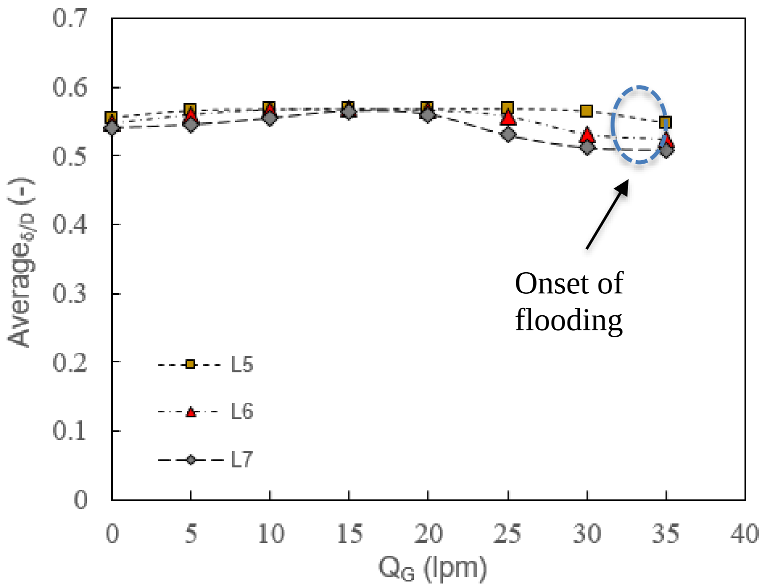

Figure 4. The effect of gas flow rate towards the average of normalized film thickness, δ/D under the flow condition of Q_L= 24 gph

Volume 5, Issue 1, pages 101-112
p-ISSN 2655-8564, e-ISSN 2685-9432

On the other hand, Fig. 5 describes the effect of liquid flow rate towards δ/D under the flow condition of Q_G= 30 gph. From the figure it can be seen that that δ/D tends to increase as the gas flow rate increases. Here, from Q_G= 14 – 20 gph, δ/D increases in which the measurement location nearest the elbow obtains the thickest liquid film. Subsequently, from Q_G= 20 – 24 lpm, δ/D increases then decreases. In addition, from Q_G= 16 – 24 gph, L5, L6 and L7 obtain an almost equal δ/D. from Q_G= 24 – 26 lpm, δ/D decreases.

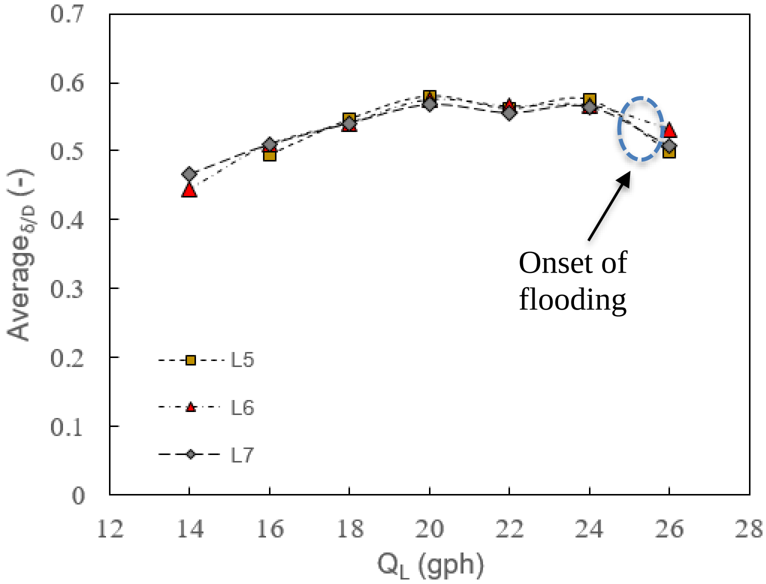

Figure 5. The effect of gas flow rate towards the average of normalized film thickness, δ/D under the flow condition of Q_G= 30 lpm

From Figs. 5-6, it can be inferred that the film thickness tends to fluctuate as the fluid flow rate increases at the subcritical region. In addition, from the visualization at the flow condition of both Q_L= 24 gph, Q_G= 35 lpm and also Q_G= 30 lpm, Q_L= 26 lpm, the limit of stability of the countercurrent flow is reached, and flooding occurs. Here the explanation is that as the fluid flow rate increases, the liquid level around the upper end of hydraulic jump increases. The following phenomena causes a narrow area for gas to pass through. Based on the momentum balance equation of horizontal countercurrent two-phase flow, the relative velocity between the phase increases. As a result, the drag force increases and causes the liquid blocks the entire cross sectional area of the conduit, and initiates flooding followed by churn. Therefore, a rather sharp decrease of δ/D is further reported to correspond to the transition from a stratified to flooding regime [16].

4 Conclusions

The behaviors of interface during gas/liquid countercurrent two-phase flow phenomena was briefly investigated. Here, a pair of fluid containing high viscous liquid/gas flows through a complex conduit representing 1/30 scaled-down of PWR hot leg's typical geometry. The flow structures were visually observed, while the film thicknesses are extracted by an image processing algorithm through the tabulated optical data. The obtained results reveal that a rather sharp decrease on liquid film thickness corresponds to the transition from a stratified to flooding regime.

Acknowledgements

The author thanks to Dr. Apip Badarudin, Dr. IGNB. Catrawedarma, Dr. Setya Wijayanta, Akhlisa Nadiantya Aji Nugroho, M.Eng., and also all members of Multiphase Flow Research Group, Laboratory of Fluid Mechanics and Heat Transfers, Department of Mechanical and Industrial Engineering, Universitas Gadjah Mada for several brief discussions during either the facility installation or particular analyses. Moreover, during a better understanding on the flow phenomenology, a Phantom Miro M310 Lab high speed camera was utilized during the experiments. Therefore, the author also acknowledges PT. Chevron Indonesia for the proper opportunity.

References

[1] Deendarlianto, T. Höhne, D. Lucas, K. Vierow, Gas-liquid two-phase flow in a PWR hot leg: A comprehensive research review, Nuclear Engineering and Design 243 (2) (2012) 214–233.

[2] Deendarlianto, C. Vallée, D. Lucas, M. Beyer, H. Pietruske, H. Carl, Erratum: Experimental study on the air/water counter-current flow limitation in a model of the hot leg of a pressurized water reactor, Nuclear Engineering and Design 241(8) (2011) 3359–3372.

[3] A. Badarudin, S. T. Pinindriya, Y. V. Yoanita, M. S. Hadipranoto, S. Hartono, R. Ariawan, Indarto, Deendarlianto, The effect of horizontal pipe length to the onset of flooding position on the air-water counter current two-phase flow in a 1/30 scale of pressurized water reactor (PWR), AIP Conference Proceedings 2001 (2018) 03001.

[4] A. Badarudin, Indarto, Deendarlianto, A. Setyawan, Characteristics of the air-water counter current two-phase flow in a 1/30 scale of pressurized water reactor (PWR): Interfacial behavior and CCFL data, AIP Conference Proceedings 1737 (2016) 040015.

[5] A. Badarudin, A. Setyawan, O. Dinaryanto, A. Widyatama, Indarto, Deendarlianto, Interfacial behavior of the air-water counter-current two-phase flow in a 1/30 scale-down of pressurized water reactor (PWR) hot leg, Annals of Nuclear Energy 116 (2018) 376–387.

[6] Deendarlianto, T. Höhne, D. Lucas, C. Vallée, G. A. M. Zabala, CFD studies on the phenomena around counter-current flow limitations of gas/liquid two-phase flow in a model of a PWR hot leg, Nuclear Engineering and Design 241(12) (2011) 5138–5148.

[7] A. H. Astyanto, Y. Rahman, A. Y. A. Medha, Indarto, Deendarlianto, Time-series differential pressure fluctuations of a flooding regime : A preliminary experimental results investigation on a 1/30 down-scaled PWR hot leg geometry, AIP Conference Proceedings 2403 (2021) 060001.

[8] A. H. Astyanto, Y. Rahman, A. Y. A. Medha, Deendarlianto, Indarto, Pengaruh Rasio I/D terhadap Permulaan Flooding dan Fluktuasi Voltase Sinyal Tekanan Rezim Flooding pada Geometri Kompleks, Rekayasa Mesin 12 (2021) 447–457.

[9] Deendarlianto, A. Ousaka, Indarto, A. Kariyasaki, D. Lucas, K. Vierow, C. Vallee, K. Hogan, The effects of surface tension on flooding in counter-current two-phase flow in an inclined tube, Experimental Thermal and Fluid Science 34(7) (2010) 813–826.

[10] Deendarlianto, A. Ousaka, A. Kariyasaki, T. Fukano, Investigation of liquid film behavior at the onset of flooding during adiabatic counter-current air-water two-phase flow in an inclined pipe, Nuclear Engineering and Design 235(21) (2005) 2281–2294.

[11] Deendarlianto, A. Ousaka, A. Kariyasaki, T. Fukano, M. Konishi, The Effects of Surface Tension on the Flow Pattern and Counter-Current Flow Limitation (CCFL) in Gas-Liquid Two-Phase Flow in an Inclined Pipe, Japanese Journal of Multiphase Flow 18 (4) (2004) 337–350.

[12] A. Ihsan, A. H. Astyanto, Indarto, Deendarlianto, Kajian Eksperimental Karakteristik Perilaku Antarmuka Aliran Berlawanan Arah di Geometri 1:30 Hot Leg PWR Menggunakan Sensor Kawat Sejajar, Prosiding Seminar Nasional Multidisiplin Ilmu Universitas Respati Yogyakarta, 3 (1) (2021).

[13] A. H. Astyanto, J. A. E. Pramono, I. G. N. B. Catrawedarma, Deendarlianto, Indarto, Statistical characterization of liquid film fluctuations during gas-liquid two-phase counter-current flow in a 1/30 scaled-down test facility of a pressurized water reactor (PWR) hot leg, Annals of Nuclear Energy 172 (2022) 109065.

[14] A. Ghoshal, A. Aspat, E. Lemos, OpenCV Image Processing for AI Pet Robot, International Journal of Applied Sciences and Smart Technologies, Vol 3 Issue 1 (2020) 65 – 82.

[15] A. H. Astyanto, A. N. A. Nugroho, Indarto, I. G. N. B. Catrawedarma, D. Lucas, Deendarlianto, Statistical characterization of the interfacial behavior captured by a novel image processing algorithm during the gas/liquid counter-current two-phase flow in a 1/3 scaled down of PWR hot leg, Nuclear Engineering and Design 404 (2023) 112179.

[16] A. H. Astyanto, Indarto, K. V. Kirkland, Deendarlianto, An experimental study on the effect of liquid properties on the counter-current flow limitation (CCFL) during gas/liquid counter-current two-phase flow in a 1/30 scaled-down of Pressurized Water Reactor (PWR) hot leg geometry, Nuclear Engineering and Design 399 (2) (2022) 112052.

This page intentionally left blank